machines

Article

Numerical Study of Flow Field Optimization for Forebay and Suction Chamber to Solve the Vibration of Pumps in a Parallel Circulation Pumping Station

Weishu Wang, Juan Zhen, Weihui Xu *, Jiawei Guo and Yuxin Zhai

School of Electric Power, North China University of Water Resources and Electric Power, Zhengzhou 450045, China
* Correspondence: xuweihui@ncwu.edu.cn

Abstract: The water inlet channel is an essential component of the thermal power plant's circulating water system. It primarily arranges the water flow in the channel so that it is introduced into the pump room smoothly, steadily, and uniformly. Significantly, the operation state of the circulating water pump is impacted by the flow condition of the water inlet channel. The coal-fired generating set's water input channel was chosen as the research object in this work, and the Computational Fluid Dynamics (CFD) Method was used to examine hydraulic issues impacting anomalous vibration of circulating pumps. Nine optimization options were also suggested, and the effects of the various plans on the water inlet channel's flow state were examined—the simulation's outcomes. The simulation's findings indicate that the arc deflector can enhance the water entry channel's flow pattern. The wall-attached bias flow of the suction chamber vanished, and the constant flow state is present around the pump's bellmouth. The thermal power unit's circulating water pump's vibration was eliminated, and the circulating pump's operating efficiency increased due to the curved deflector's rectification procedures being implemented in the forebay. The study's findings can guide the hydraulic performance optimization of channels for water inlets with similar sideways or high slopes.

Keywords: forebay; hydraulic characteristics; numerical simulation; pump vibration; rectification optimization; suction channel

Citation: Wang, W.; Zhen, J.; Xu, W.; Guo, J.; Zhai, Y. Numerical Study of Flow Field Optimization for Forebay and Suction Chamber to Solve the Vibration of Pumps in a Parallel Circulation Pumping Station. *Machines* **2022**, *10*, 680. https://doi.org/10.3390/machines10080680

Academic Editor: Antonio J. Marques Cardoso

Received: 30 June 2022
Accepted: 6 August 2022
Published: 11 August 2022

1. Introduction

The circulating water system is essential to a thermal power plant's water supply system. After heat exchange, the low-enthalpy cooling water is pumped into the circulating cooling water system by circulating water pumps [1]. The water inlet channel connects the pump room and the pond, consisting of the diversion section, the forebay, and the suction chamber. A suitable flow pattern must be created in the water inlet channel to ensure that the fluid flows smoothly into the suction chamber. The forebay is a vital component of the water inlet channel. Its primary function is to smoothly direct water flow into the circulating pump [2]. The flow state of the pumping station forebay directly impacts hydraulic performance and operational efficiency. The hydraulic performance, operating efficiency, and service life of the circulating pump are all directly affected by the flow state of the pumping station forebay [3,4]. Bad flow states, such as bias and wall-to-wall flow, occur in some irregularly designed inlet water passages. These poor flow states are the hydraulic causes of the circulating pump's vibration [5]. The vibration reduces circulating pump performance, which damages flow channel components and jeopardizes the pumping station's safety [6].

In recent years, Computational Fluid Dynamics (CFD) has become a standard research tool to improve analysis efficiency and study the flow field in more realistic detail. Many scholars worldwide have used the turbulence model to conduct a series of studies on the flow regime of water inlet channels and have produced fruitful results. Luo et al. [7]

used a Realizable turbulence model, and Reynolds-averaged Navier–Stokes equations (N–S equations) to study the forebay's flow pattern without optimization measures. His research shows that the forebay's flow pattern can be significantly improved by adjusting the bottom sill's shape. Han et al. [8] created a 3D model of the entire flow channel and ran numerical simulations using the Renormalization Group (RNG) turbulence model. This method simulated the hydraulic characteristics of steady and transient flow in the forebay. Zhou et al. [9] chose Reynolds-averaged N–S equations and a standard turbulence model to simulate the flow pattern in the forebay numerically. They also analyzed and determined the influence of the diversion wall's rectification scheme on the flow pattern in the forebay. Xu et al. [10] used FLUENT to simulate the flow pattern of the forebay and proposed antideposition measures for the diversion pier and pressure plate. After the measures were implemented, backflow and deposition on both sides of the forebay decreased.

At present, Numerous real-world engineering issues have currently been resolved through numerical simulation. Diagnosing and optimizing hydraulic issues in circulating water systems frequently employ numerical simulation technology. The study's findings demonstrate that numerical simulation studies accurately reflect the actual situation. The lateral inlet flow channel's flow characteristics and rectification principles were researched by Cheng et al. [11], and various optimization techniques were applied to improve the flow pattern. The measures listed by Wang et al. [12] for optimizing the flow conditions in the forebay were choosing the bottom diversion pillar, adding a pier diversion pillar, and setting the water pressure plate and diversion pier. These measures were combined with engineering practice. They also detailed the merits and cons of various strategies and examined and compared various optimization measures. In addition to simulating and researching the pumping station's diversion characteristics in the Tianshan Irrigation District, Liu et al. [13] have proposed several reconstruction strategies. The findings indicated that the pressure plate and discontinuous bottom sill combination was the optimal strategy for flow correction in the forebay. Yang et al. [14] analyzed the flow field in the forebay of a multimachine pumping station. Based on model tests and numerical simulation, they selected different rectification measures to adjust the flow pattern in the forebay. The combination plan of the rectifier bucket and the diversion wall hole was the best. Ying et al. [15] analyzed the flow pattern in the forebay by using the volume of fluid (VOF) and put forward the optimization measures. The results show that the rectification effect of the diversion pillar–sill combination layout plan was the best, and the flow distribution was more uniform with the help of a diversion pillar arrangement and a modification to the sidewall boundary profile. Xu et al. [16] adjusted the flow states of the forebay. The results indicate that the optimization plan completely removed the disordered flow close to the forebay's large-scale reflux area due to the issues with the forebay's concentrated main stream, high flow velocity, reflux zone, and uneven water inflow. The concept of a "multi herringbone" combined forebay diversion pier was proposed by Bai et al. [17]. The water flow is distributed by this strategy, reducing the forebay's reflux zone and mainstream flow velocity. Zhou et al. [18] examined the flow pattern of the circulating water channel using numerical simulation with the traditional k-turbulence model and assessed the impact of various forebay combination sizes on the flow field.

In the paper, researchers used Computational Fluid Dynamics (CFD) to study the pump vibration and the flow field law of the water channel by consulting the design data and site survey. The hydraulic performance of the overall flow channel in the original design plan was improved and optimized. Various optimized rectification plans were proposed, and the best rectification measures were selected and successfully practiced, which can provide a reference for similar engineering examples.

2. Research Background

The circulating water system in this research object includes an atmospheric cooling tower and a room for the unit's circulating water pump. In the pump room, three circulating pumps are set up. The circulating pump is an induction motor-driven diagonal pump with an adjusted speed and fixed vane. The circulating pump, on the other hand, is made up of a spiral casing, a bladed disk, a shaft and bearing, a shaft gland, etc. The circulating pump operation condition is shown in Table 1.

Table 1. Circulating pump operation condition table.

Operating Mode of Circulating Water Pump	High-Speed Operation of Three Pumps	Low-Speed Operation of Three Pumps	High-Speed Operation One Pump	Low-Speed Operation One Pump
Flow (m^3/s)	28.77	25.65	9.59	8.55

Pump efficiency: during high-speed operation $\eta \geq 89\%$; during low-speed operation $\eta \geq 87\%$.

Since the unit of the thermal power plant was put into operation, abnormal vibration of the circulating pump was found many times. Therefore, the circulating pump was disassembled and overhauled, and the following problems were found during the repair:

(1) The bearing of the circulating pump had a partial grinding phenomenon;
(2) Deflection of the outlet extension element in the circulating pump;
(3) The blade disk and the blade disk chamber also showed the phenomenon of partial grinding.

The vibration situation was not wholly solved after maintenance. These problems prevent the circulating water pump from running at a high speed.

Aiming at various problems in the operation of circulating pumps, maintenance staff reinforced the pump barrel with steel pipes and fixed it with four steel pipes. After increasing the strength of the pump barrel connector, the vibration of the circulating pump was partially improved, but abnormal vibration appeared again after running for some time. Therefore, it is a critical study to find the root cause of the vibration in the circulating pump. Only by understanding the root cause of the vibration of the circulating pump can the problem of vibration be fundamentally solved.

3. Mathematical Formulation

The circulating water flow is an incompressible fluid and constant flow, and heat transfer is not considered during operation. The governing equation of the numerical simulation calculates based on the Reynolds-averaged Navier–Stokes equations. The Realizable $k-\varepsilon$ model is used to enable the N–S equations to be closed.

3.1. Equation of Continuity

The continuity equation are partial differential equations that describe the transport behavior of conserved quantities. Its expression is as follows.

$$\frac{\partial u_i}{\partial x_i} = 0 \tag{1}$$

where (u_i) is the velocity vector in the i direction and x_i (i = 1,2,3) is the coordinate axis.

3.2. Momentum Equation

The momentum equation is the expression of the law of conservation of momentum in fluid mechanics. Its expression is as follows.

$$u_j\frac{\partial u_i}{\partial x_j} + \frac{1}{\rho}\frac{\partial p}{\partial x_i}\frac{\partial}{\partial x_j}\left[(\nu+\mu_t)\left(\frac{\partial u_i}{\partial x_j}+\frac{\partial u_j}{\partial x_i}\right)\right] = f_i \tag{2}$$

where x_i is also the coordinate axis; ρ is the density of liquid, kg/m^3; p is Pressure, Pa; ν is the kinematic viscosity coefficient of water, m^2/s; μ_t is eddy viscosity coefficient, m^2/s; and f_i is the mass force along i direction;

3.3. Turbulence Models

Turbulent kinetic energy equation:

$$\frac{\partial}{\partial t}(\rho k) + \frac{\partial}{\partial x_j}(\rho k u_j) = \frac{\partial}{\partial x_j}\left[\left(\mu + \frac{\mu_t}{\sigma_k}\right)\frac{\partial k}{\partial x_j}\right] + G_k - \rho\varepsilon \tag{3}$$

Dissipative differential equation:

$$\frac{\partial}{\partial t}(\rho\varepsilon) + \frac{\partial}{\partial x_j}(\rho\varepsilon u_j) = \frac{\partial}{\partial x_j}\left[\left(\mu + \frac{\mu_t}{\sigma_\varepsilon}\right)\frac{\partial \varepsilon}{\partial x_j}\right] + \rho C_1 S\varepsilon + \rho C_2 \frac{\varepsilon^2}{k + \sqrt{\nu\varepsilon}} \tag{4}$$

In these equations: k is turbulent kinetic energy, m^2/s^2; ε is the turbulent dissipation rate, m^2/s^3; G_k represents the turbulent kinetic energy generated by the average velocity gradient; C_1 and C_2 are constants with values of 1.44 and 1.92 respectively; σ_k and σ_ε are turbulent Brandt numbers of k and ε with values of 1.0 and 1.3 respectively.

3.4. VOF Fluid Interface and Free Surfaces

The phenomenon of flow with free surfaces is common in nature, for example, the flow of the inlet channel of the open pumping station, the flow of the tide, and the flood flow of dam failure. The difficulty in numerical simulation of this flow with a free surface is the tracking of the free surface.

Currently, VOF is mainly used to simulate the flow of the free surface. The model introduces volume fraction variables for each phase and determines the interface between phases by solving the volume fraction in each control unit. Therefore, if the water–gas two-phase field α_w represents the volume fraction of water, then the volume fraction of gas can be expressed as $\alpha_a = 1 - \alpha_w$.

The value α_w knows the location of the free surface of. However, this project has a defined free water surface location, which can be given directly. The elevation at 8 m is set as the free liquid surface.

4. Numerical Simulation

4.1. Three-Dimensional Model

In order to accurately simulate the flow process, a full-channel and circulating pump model were established. Figure 1 is the structure diagram of the circulating pump. Figure 2 shows the arrangement of the pump.

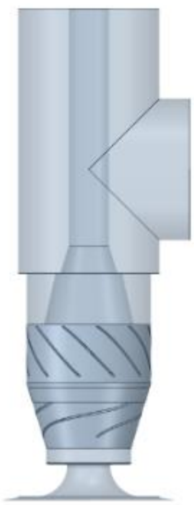

Figure 1. Circulating pump structure.

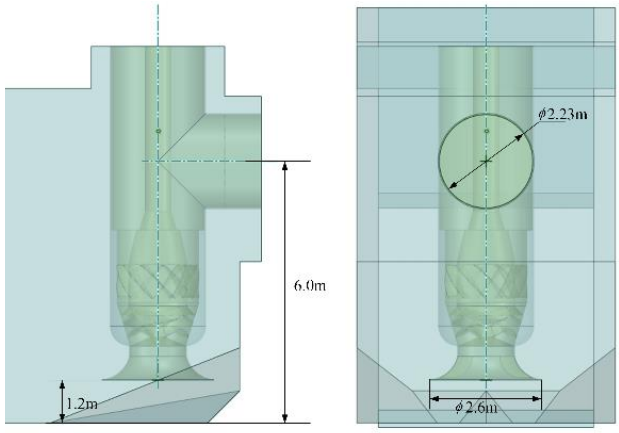

Figure 2. The arrangement of the pump.

The water inlet channel structure is shown in Figure 3. The water flow in the cooling tower enters the channel diversion from the inlet; the channel diversion consists of two arc-shaped water channels separated symmetrically in the middle. After the water passes through the open forebay, the water flow enters the A, B, and C water suction chambers separated by unit, then the circulating pump in the water suction chambers pumps water into the drainage pipeline. The operating water level of the water suction chamber is 8 m; one pump has a flow rate of 9.59 m^3/s and is ahead of 28.65 m. The summer operation condition is adopted in the simulation. That is, three pumps run simultaneously.

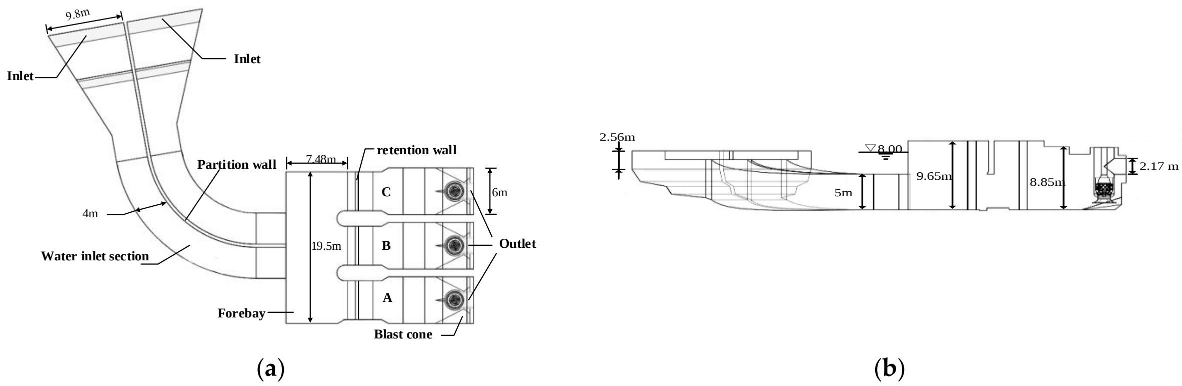

Figure 3. Structure diagram of inlet channel. (**a**) Vertical view. (**b**) Lateral view.

4.2. Mesh Subdivision

4.2.1. Meshing Technology

The meshing of the physical model is based on the FluentMeshing 2020R2 software (Wayne Smith, Canonsburg, PA, USA). A hybrid mesh was used, the polyhedral mesh was used at the boundary, and the hexahedral mesh was used inside. The hybrid grid reduces the number of grids and improves the mesh accuracy, which can ensure the calculation accuracy of the circulating pump operation. Considering the influence of the wall surface on the flow field in the circulating pump, refine the mesh of the circulating pump section. The mesh model diagram is shown in Figure 4.

4.2.2. Mesh Independence Verification

The finer the mesh is divided, the higher the accuracy of the solution results. However, the increase in the number of meshes leads to a significant increase in the time cost of computation, and the improvement of computational accuracy is not apparent when the number of meshes reaches a specific number. Therefore, it is necessary to compare the calculation results under the conditions of the different number of meshes and judge the irrelevance of the results to the meshes. The inlet condition of the circulation pump bellmouth is the main parameter to judge the pump's vibration, so the average velocity of both sides of the C circulation pump is chosen as the comparison parameter to determine the independent mesh results.

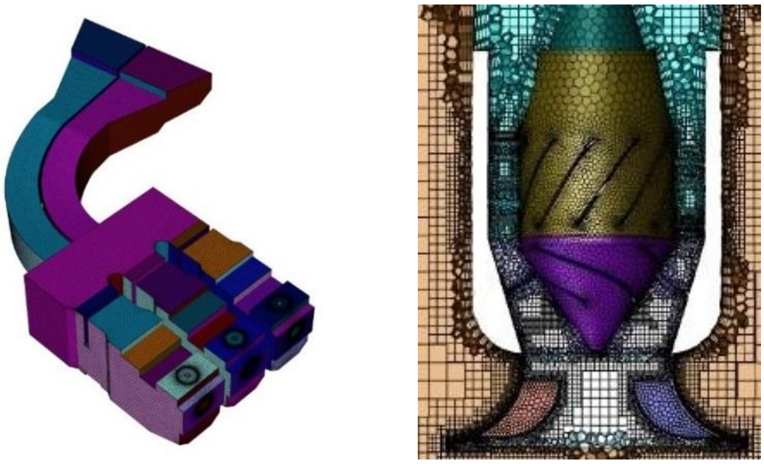

(**a**) (**b**)

Figure 4. Mesh model of inlet channel. (**a**) Overall mesh. (**b**) Refined mesh.

Figure 5 shows the results of mesh independence verification. Each mesh number is 2.0 million, 3.02 million, 4.2 million, 5.03 million, and 6.1 million, respectively. The result shows that when the mesh number exceeds 4.2 million, the change in average velocity is not apparent. It can be considered that the calculation results are independent of the mesh. Therefore, the 4.2 million mesh model was selected for calculation.

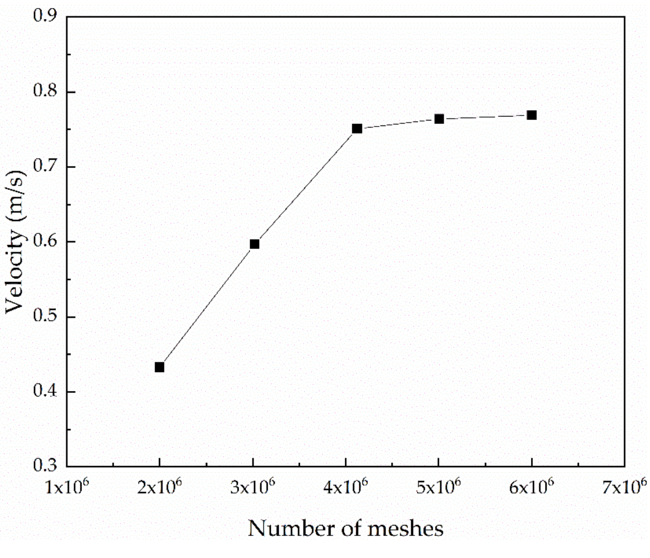

Figure 5. Mesh independence verification.

4.3. Boundary Conditions and Calculation Method

FLUENT 2020R2 software (Boysan, Canonsburg, PA, USA) was used for this calculation, selecting Pressure Solver and Steady-State Solver. The Realizable $k - \varepsilon$ turbulence model was selected, and the Upwind Difference Equation was adopted for implicit solving. Meanwhile, the SIMPLE algorithm was used for pressure–velocity coupling. The nonslip conditions $u = 0, v = 0$ and $w = 0$ are used for the inner wall of the water flow channel.

Boundary conditions according to the actual operating conditions in summer: three pumps run at the same time, and the total flow rate is 28.77 m^3/s. The circulating pump is rotated by Moving Reference Frame and rotates at 370 r/min. The VOF model was used for the water-free surface; then, the initial liquid level was given as the elevation of 8. The pressure outlet is adopted at the top of the forebay; the pressure value is atmospheric pressure. In the meantime, the channel's inlet flow rate and outlet flow rate are given to keep the liquid level stable.

4.4. Rectification Plan

Many researchers have conducted rectification optimization research on the forebay of thermal power plants. Standard flow rectification plans for inflow channels include:

(1) Set diversion blocks, deflectors, or diversion pillars in the forebay;
(2) Set bottom levee in the forebay;
(3) Refill the forebay and replace the rectangular forebay wall with trapezoidal, polygonal, or curved forebay walls;
(4) Set deflection cone in suction chambers.

Among them, setting the bottom levee and backfilling the forebay are mainly used to eliminate the vortex in the forebay. However, the construction volume of this plan is significant; the current optimization does not select this plan as the optimization scheme. Since the suction chamber already has deflection cones in the original design, the plan of setting the deflection cones below the water inlet of the circulating pump is not considered. Meanwhile, the diversion measures such as deflectors or diversion pillars have a significant rectification effect, easy structure control, and minor construction amount. Therefore, the paper chooses the deflector as the basis for the optimization design research.

According to the characteristics of the model, three kinds of deflectors were set: diversion pillar, linear deflector, and arc deflector. A total of nine optimization plans have been designed. The setting mode of deflectors is shown in Table 2.

Table 2. Flow-diverting plate plans setting table.

Plan	Plan Description	Action Description
1	Original plan	No rectification measures
2	Linear deflector	Two linear deflectors are arranged on both sides of the forebay, with a height of 4 m. The shape and arrangement of rectification measures are shown in Figure 6a.
3	Diversion pillar	Six diversion pillars on both sides of the forebay with a height of 2 m. The shape and arrangement of rectification measures are shown in Figure 6b.
4	Arc deflector	Two arc deflectors are arranged on both sides of the forebay with a height of 4 m. The shape and arrangement of rectification measures are shown in Figure 6c.
5	Linear deflector	Three linear deflectors are set in the forebay with a height of 5 m, the middle plate is perpendicular to the inlet of the forebay. The shape and arrangement of rectification measures are shown in Figure 6d.
6	Linear deflector	Three linear deflectors are set in the forebay with a height of 5 m. The shape and arrangement of rectification measures are shown in Figure 6e.
7	Arc deflector	Three deflectors are set in the forebay with a height of 3 m. The deflectors with an arc of 45° are on both sides of the forebay. The shape and arrangement of rectification measures are shown in Figure 6f.
8	Arc deflector	Three deflectors are set in the forebay with a height of 3 m. The deflectors with a radian of 40° are on both sides of the forebay. The shape and arrangement of rectification measures are shown in Figure 6g.
9	Arc deflector	Three deflectors are set in the forebay with a height of 3 m. The deflectors with a radian of 35° are on both sides of the forebay. The shape and arrangement of rectification measures are shown in Figure 6h.
10	Arc deflector	There are three deflectors in the forebay with a height of 4 m. The deflectors with a radian of 35° are on both sides of the forebay. The shape and arrangement of rectification measures are shown in Figure 6i.

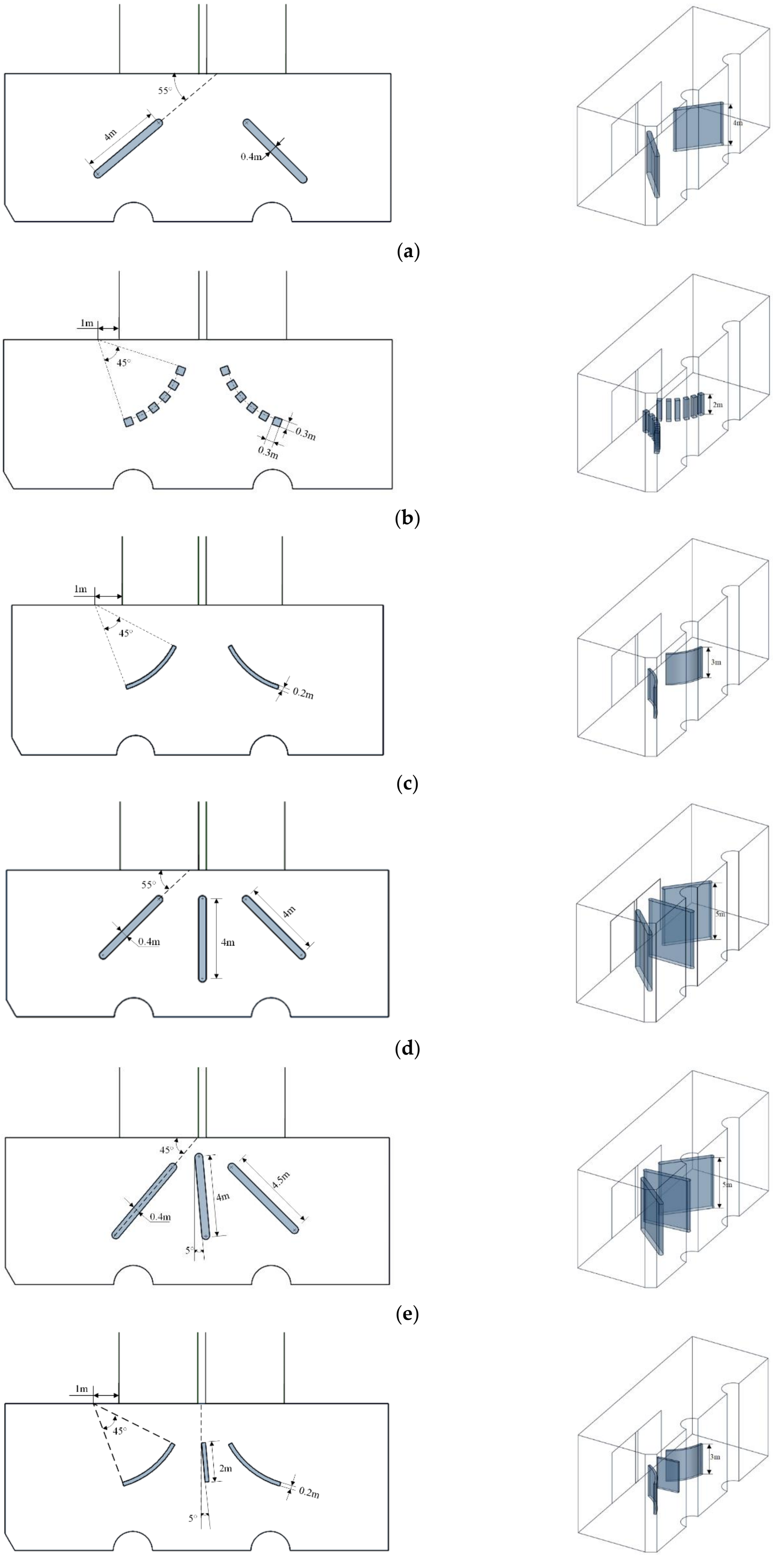

Figure 6. *Cont.*

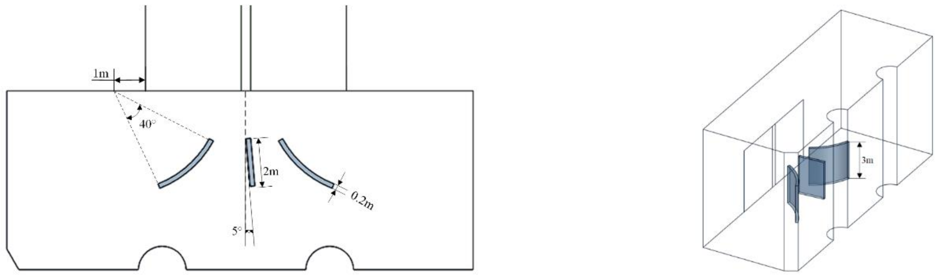

(**g**)

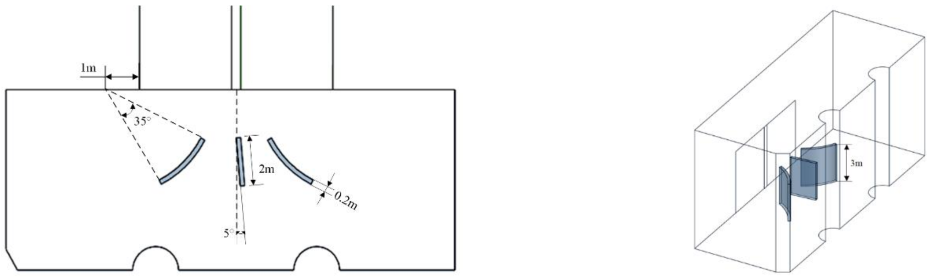

(**h**)

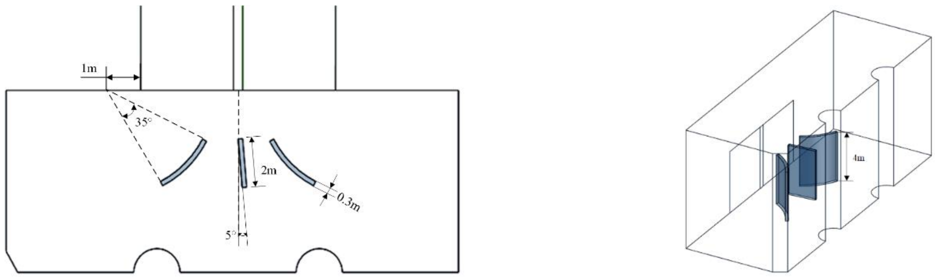

(**i**)

Figure 6. Forebay renovation diagram. (**a**) Plan 2. (**b**) Plan 3. (**c**) Plan 4. (**d**) Plan 5. (**e**) Plan 6. (**f**) Plan 7. (**g**) Plan 8. (**h**) Plan 9. (**i**) Plan 10.

The following Figure 6 is a schematic diagram of the forebay renovation under different rectification measures. The shape and quantity of the diversion pillar and the deflector are shown in the Figure.

5. Results and Discussion

5.1. Analysis of Original Working Condition

The characteristic section fully considers the hydraulic characteristics and flow regime of the entire circulating water channel. The analysis of each characteristic section can comprehensively summarize the circulating water channel's overall flow field and flow regime. Figure 7 is the velocity vector of the characteristic section at 0.6, 1.2, and 2 m under the original design condition. The height of the characteristic section is based on the bottom of the forebay.

It can be seen in Figure 7 that the circulating water flows into the forebay through the arc section channel. Since the angle of the arc-shaped channel is close to a right angle, the flow velocity of the water flow on one side of the flow channel is relatively high, and a high-speed water flow area is formed at the forebay. In addition, due to the short length of the forebay and the large inflow diffusion angle, the high-speed water flow cannot be sufficiently buffered, so the water flow in the forebay is not fully developed and unevenly developed, and bias still exists in the water flow and high-velocity area after entering the suction chambers. There are apparent deviations in the water flow distribution of the suction chambers. The high-speed water flow in the two suction chambers A and C flows close to the inner wall, resulting in a large water velocity and water pressure on the single sidewall. The suction chamber of B faces the water outlet of the arc-shaped water channel, and the high-speed water flow quickly impacts the front edge of the bellmouth of the B circulating pump.

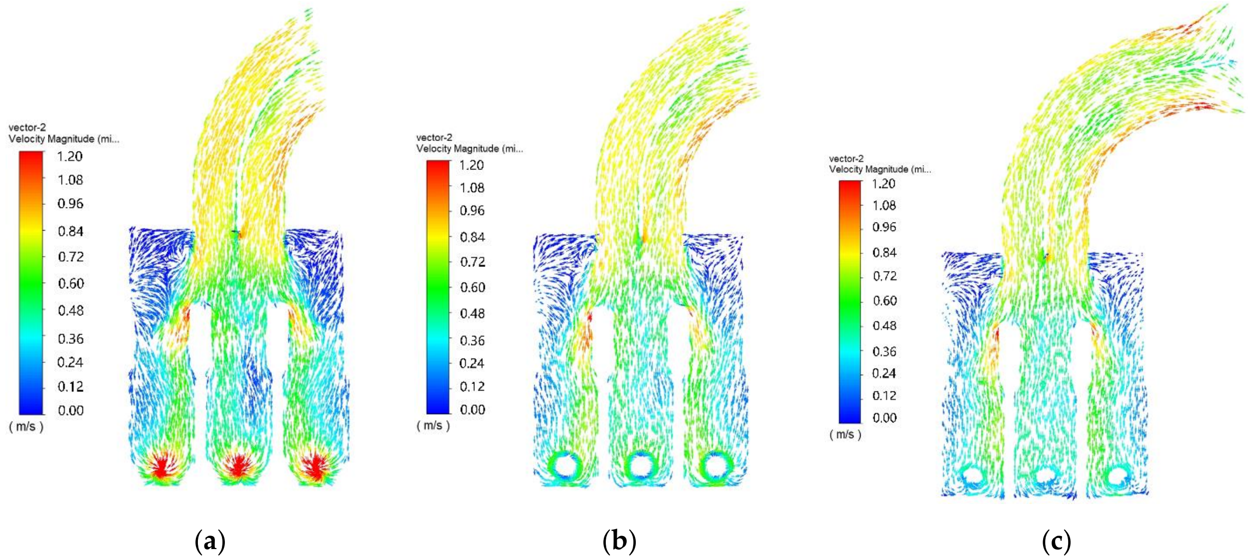

Figure 7. Velocity vector of the characteristic section of the water channel in original design. (**a**) 0.6 m sectional view. (**b**) 1.2 m sectional view. (**c**) 2 m sectional view.

It can be seen from Figure 8 that the deviation of the water flow after entering the pump room results in a very uneven distribution of the flow velocity around the bellmouth of the circulating pump. Especially for the two circulating pumps, A and C, the maximum flow rate is about 1 m/s, and the flow rate difference between the front and rear edges of the A circulating pump is 0.7 m/s, which is very unfavorable to the stable operation of the circulating pumps. Poor flow regimes cause the variable flow rate in the forebay and pump room. The hydraulic problem caused by the variable flow rate is the main reason for the abnormal vibration of the circulating pumps.

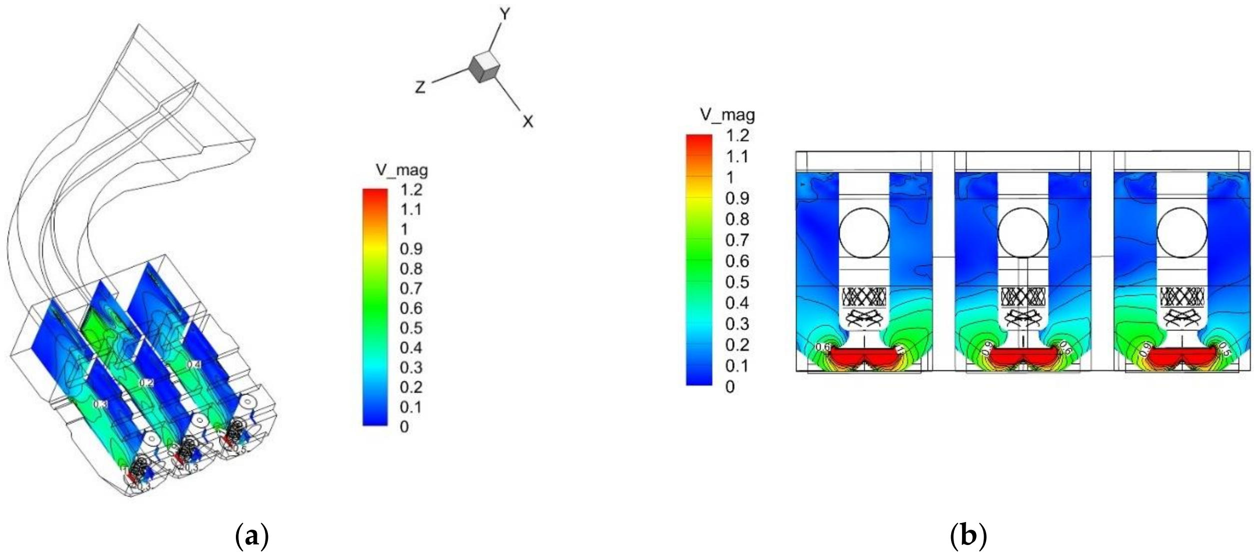

Figure 8. Plan 1 isogram of velocity. (**a**) Center section of pump body along flow direction. (**b**) Center section of pump body in vertical flow direction.

5.2. Overall Flow Field Analysis of Each Plan

A critical judgment that affects the vibration of the circulating pump is the uniformity of the flow field around the bellmouth of the circulating pump. Therefore, by analyzing the flow field distribution of the characteristic cross-section at 1.2 m of different reconstruction plans, the effect of the reconstruction plan can be clearly understood.

It can be seen from Figure 9a that compared with the original working condition, Plan 3 has been better improved. However, there is still a slight drift in the A and C pump rooms, but the overall transformation effect is not harmful. In addition, the modification of the installation of the arc-shaped deflector in Plan 4 has dramatically improved. However, the diversion effect is vital so that the water flow enters from the outside of the A and C pump rooms, and there is also a slight deviation, but the overall transformation effect is better.

It can be seen from Figure 9d that the diversion effect of the linear deflector is not as good as that of Plans 3 and 4. The modification of Plan 5 generates small vortexes in the forebay and pump rooms A and B, causing the water flow to hit the wall and drift, which is very unfavorable for the regular operation of the circulating pump. In addition, the setting of the inclined middle plate in Plan 6 improves the water flow entering the C pump room compared with the original working condition, but the bias flow of the A pump room changes from the inside to the outside, and the B pump room also has partial flow.

The above analysis shows that the inclined middle plate transformation is feasible, but the flow state in pump rooms A and B needs further improvement.

It can be seen from the Figure 9 velocity vector that the transformation of the arc-shaped deflector dramatically improves the uniformity of the water flow entering each pump room, but the diversion effect of Plans 7 and 8 is vital so that the water flow does not enter from the middle of the pump room. Comparing Plan 10 and Plan 9, it can be seen that after the radian of the arc deflector is continuously reduced, the uniformity of the flow field is greatly improved. At the same time, after increasing the height of the deflector, the overall flow field of Plan 10 is more uniform than Plan 9, the bias flow disappears, and the transformation effect is good.

From the above analysis, Plans 4, 8, 9, and 10 have better improvement for the biased current situation compared with the original working condition. However, to evaluate the pros and cons of the water inlet conditions of the circulating pump, it is not simply to look at the uniformity of the overall flow field but also to consider the uniformity of the water flow velocity around the circulating pump, especially the uniformity of the water flow around the bellmouth of the circulating pump.

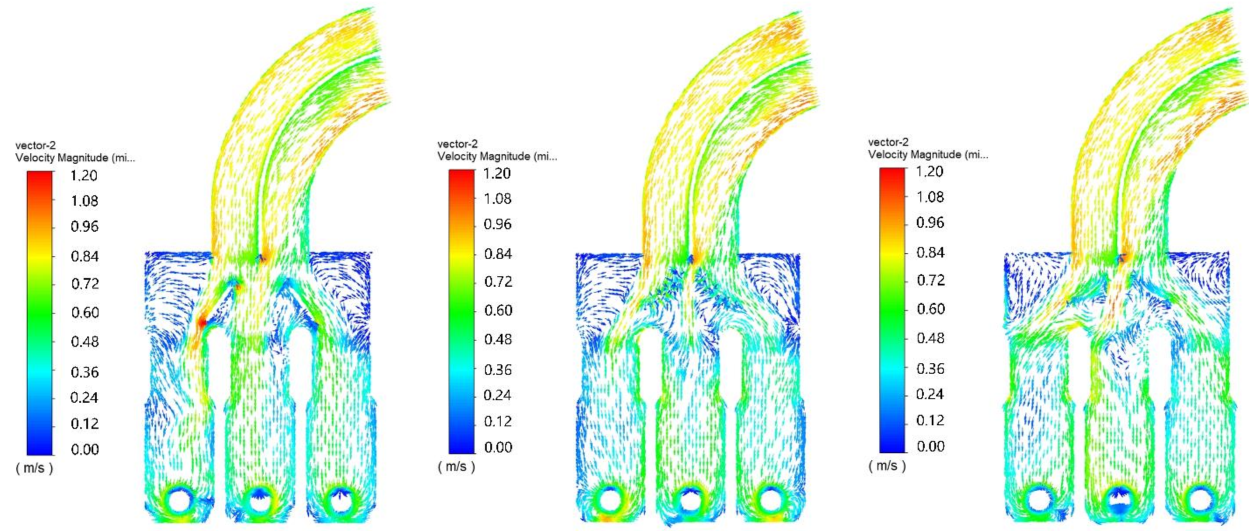

(**a**) (**b**) (**c**)

Figure 9. *Cont*.

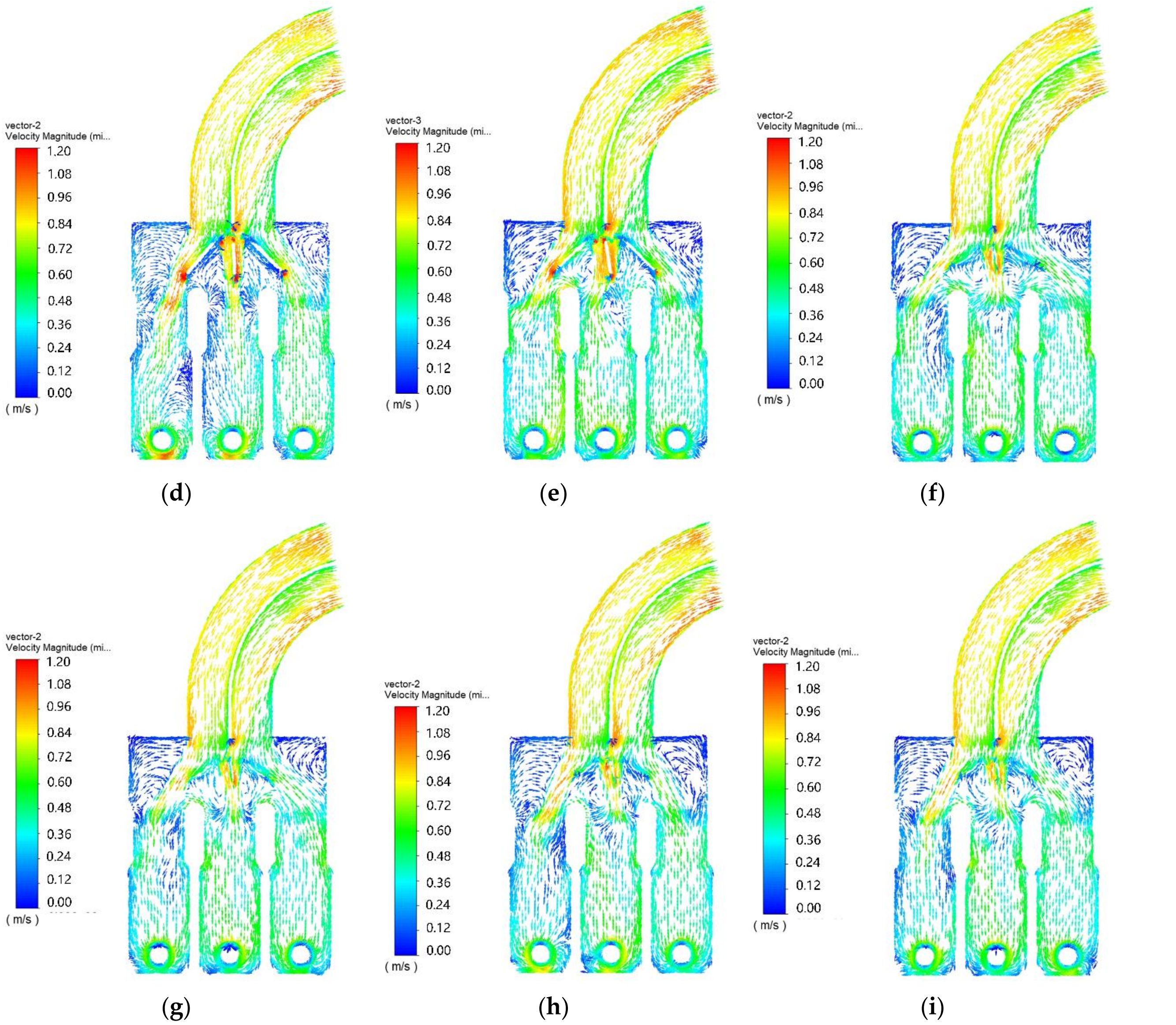

Figure 9. Velocity vector of overall flow field at 1.2 m. (**a**) Plan 2. (**b**) Plan 3. (**c**) Plan 4. (**d**) Plan 5. (**e**) Plan 6. (**f**) Plan 7. (**g**) Plan 8. (**h**) Plan 9. (**i**) Plan 10.

5.3. Hydraulic Performance Analysis of Recirculation Pump Bellmouth

Another critical judgment that causes pump vibration is the distribution of water flow velocity near the bellmouth of the circulating pump. Whether the flow velocity around the bellmouth is uniform is critical to the stable operation of the circulating pump. Next, the flow velocity distribution near the bellmouth of the circulating pump is analyzed for different improvement plans.

According to the Plan 2 central isogram of each pump room in Figure 10a, the water flow velocity from the forebay into the suction chambers was partially increased, especially in pump room A. The flow velocity difference between the front and rear edges of the circulating pump bellmouth is also significant. In addition, it can be seen from Figure 10b that the speed difference between the left and right sides of the C circulating pump bellmouth becomes smaller, while the flow velocity difference between the A and B circulating pumps bellmouth becomes larger. This situation is also not conducive to the stable operation of the circulating pump.

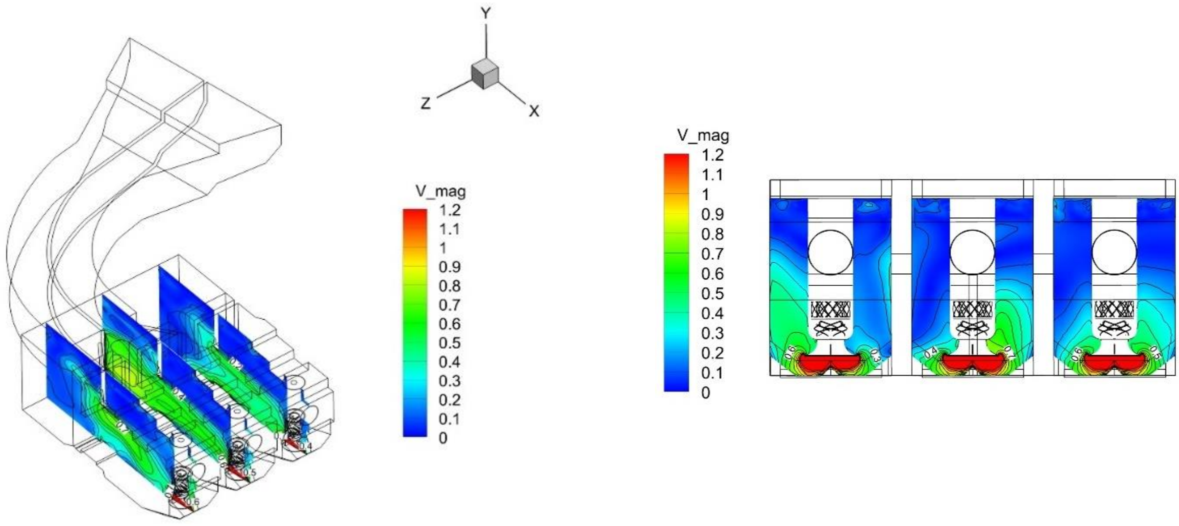

(a) (b)

Figure 10. Plan 2 isogram of velocity. (**a**) Center section of pump body along flow direction. (**b**) Center section of pump body in vertical flow direction.

According to the Plan 3 center isogram of each pump room in Figure 11a, pump room B faces the outlet of the arc-shaped water channel, and pump room B is located in the middle of the columns on both sides. These result in a partial increase in the velocity of the water flow into pump room B. In addition, the flow velocity difference between the front and rear edges of the circulating pump bellmouth is enormous, especially the front speed of the A and C circulating pump bellmouths, which are as high as 1, which is very unfavorable for the operation of the circulating pump. At the same time, from Figure 11b, it can be seen that the flow rates on the right side of the circulating pumps A and B are more extensive than those on the left side, and the C circulating pump does not change. The transformation effect of this Plan 3 is poor.

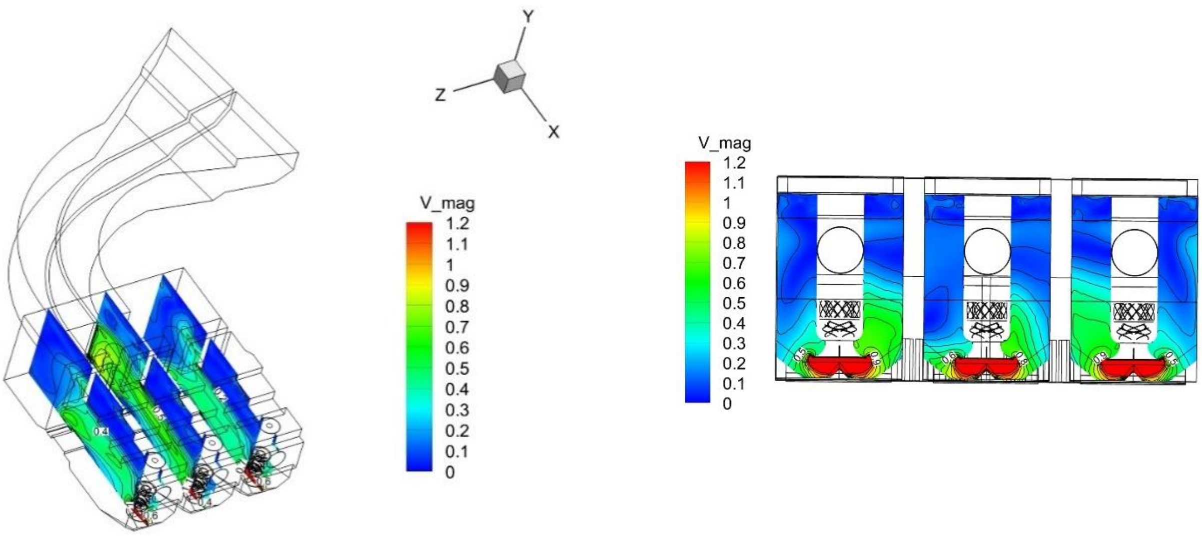

(a) (b)

Figure 11. Plan 3 isogram of velocity. (**a**) Center section of pump body along flow direction. (**b**) Center section of pump body in vertical flow direction.

It can be seen in Figure 12a that the situation of Plan 4 is similar to Plan 3. The pump room B is located in the middle of the two arc-shaped deflectors; the water flow speed is then partially increased. In addition, the flow velocity difference between the front and rear edges of each circulating pump is relatively significant, which is easy to cause the circulating pump to vibrate. At the same time, it can be seen from Figure 12b that the flow velocity difference between the left and right sides of the A and B circulating pump bellmouths have decreased, but there is still a difference in the condition of the C circulating pump, which has deteriorated. The analysis shows that the transformative effect of this scheme is poor.

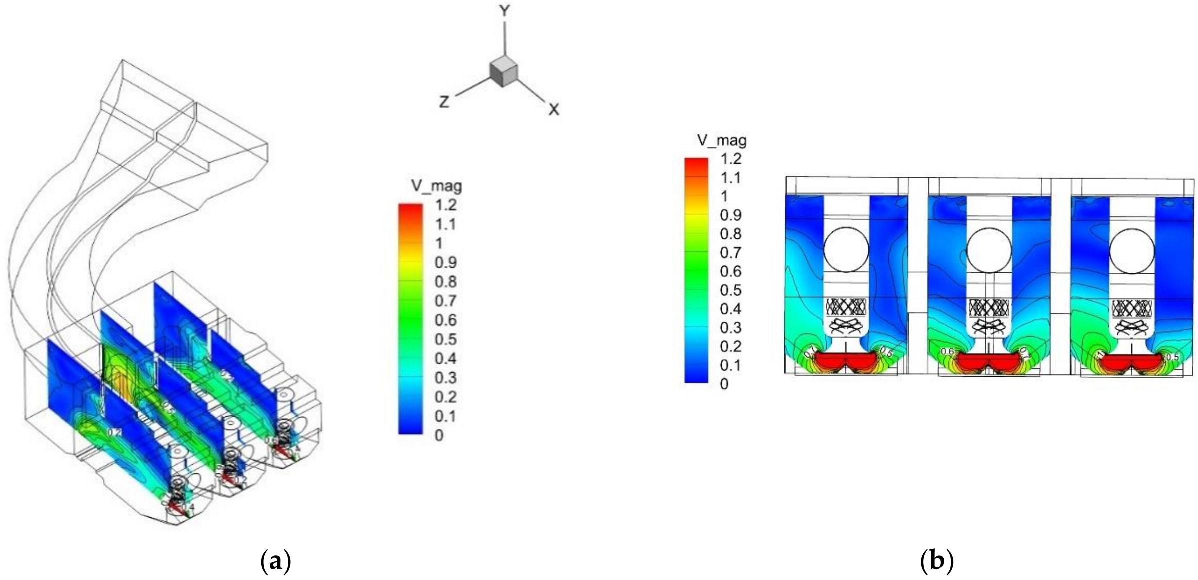

Figure 12. Plan 4 isogram of velocity. (**a**) Center section of pump body along flow direction. (**b**) Center section of pump body in vertical flow direction.

Compared with Plan 5, the middle deflector is deflected to the right by 5° in Plan 6. From the above Figures 13 and 14, it can be seen that the middle flow equalizing plate plays a role in diverting the water flow. After the diversion, the water flow into each pump room is equal, and the high-velocity area is reduced, but the bias flow still exists.

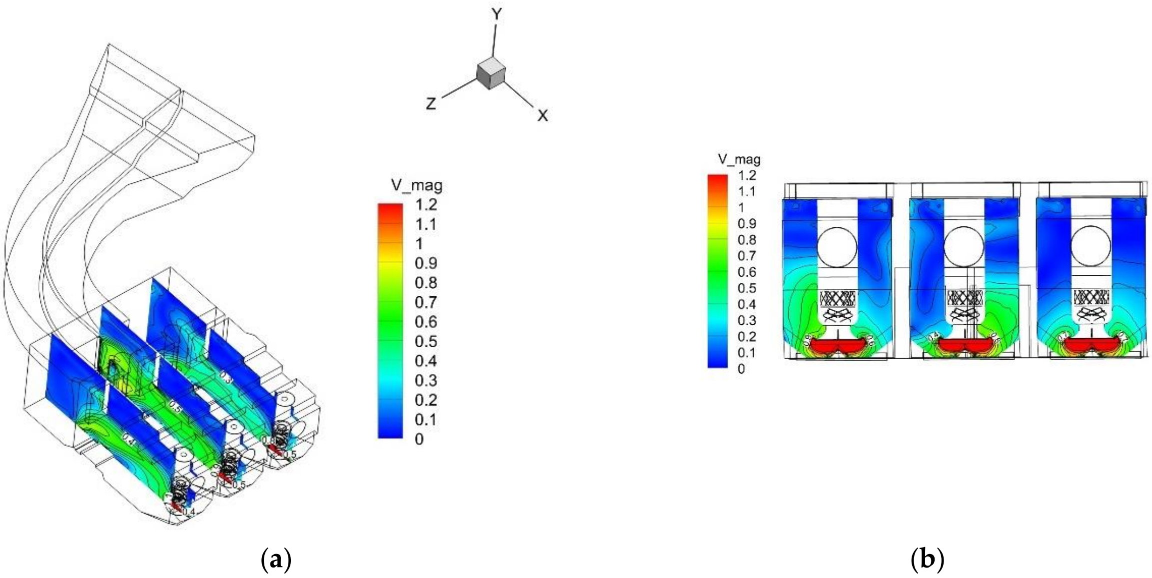

Figure 13. Plan 5 Isogram of velocity. (**a**) Center section of pump body along flow direction. (**b**) Center section of pump body in vertical flow direction.

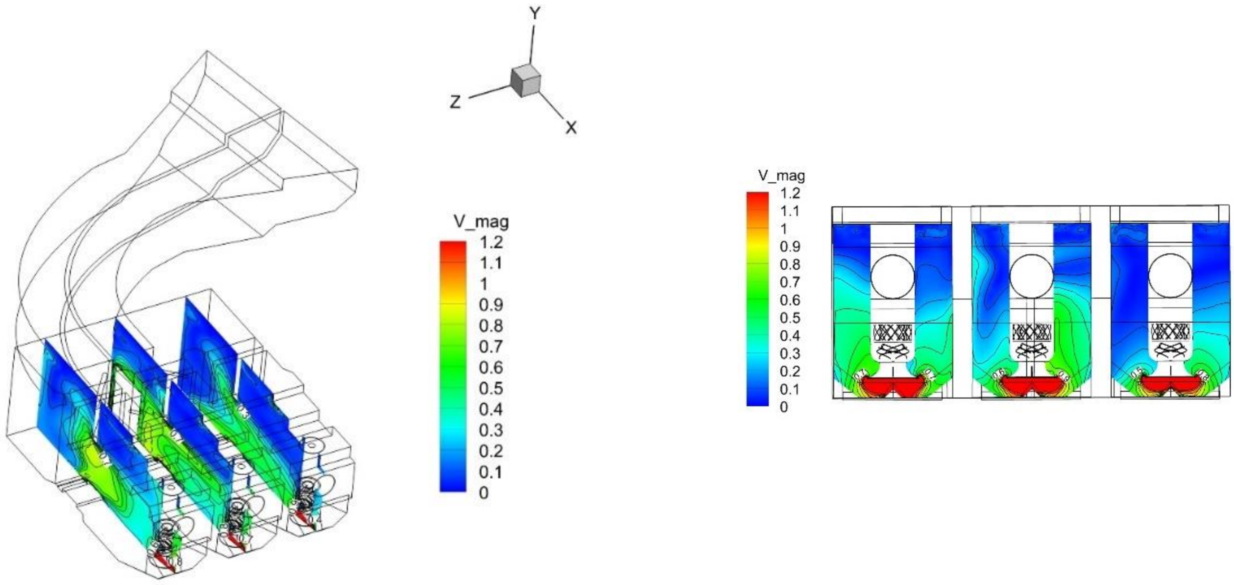

(**a**) (**b**)

Figure 14. Plan 6 isogram of velocity. (**a**) Center section of pump body along flow direction. (**b**) Center section of pump body in vertical flow direction.

Plan 7 and Plan 8 are, respectively, optimized plans for arc-shaped deflectors with radians of 45° and 40°. From the comparison of Figures 15a and 16a, it can be seen that the solution with a radian of 45° has a strong deflection effect, so the water flow after entering the pump room still has a little flow. However, the bias current is partially improved after reducing the arc to 40°.

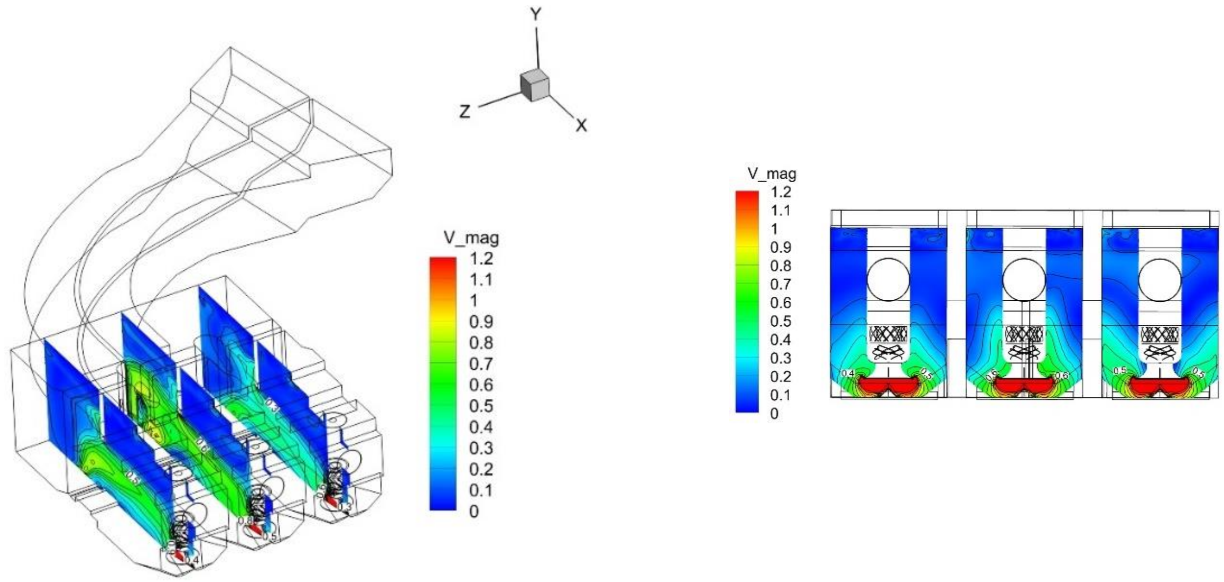

(**a**) (**b**)

Figure 15. Plan 7 Isogram of velocity. (**a**) Center section of pump body along flow direction. (**b**) Center section of pump body in vertical flow direction.

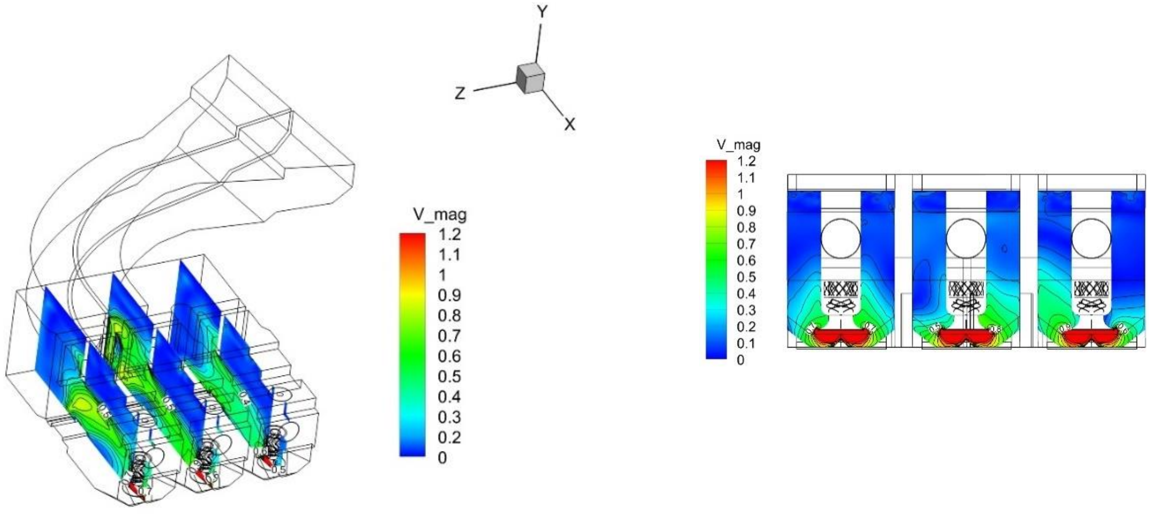

(**a**) (**b**)

Figure 16. Plan 8 isogram of velocity. (**a**) Center section of pump body along flow direction. (**b**) Center section of pump body in vertical flow direction.

In Plan 8, the difference in water flow velocity between the front and rear edges of the circulating pump bellmouths is partially improved. In addition, from Figures 15b and 16b, it can be seen that the improvement effect of the arc deflector on the flow velocity of the left and right sides of the circulating pump bellmouth is better than that of the Plan 5.

Plans 9 and 10 are the improvement of the arc-shaped deflectors with the same radian of 35° but different heights and widths. Compared with Plan 8, the uniformity and stability of the flow state are greatly improved after the radian is further reduced to 35°. It can be seen in Figures 17a and 18a that the flow velocity difference between the front and rear edges of the circulating pump bellmouth is minimal. From the comparison between Figures 17b and 18b, increasing the height of the deflector can improve the flow velocity difference between the left and right sides of the circulating pump bellmouth. As can be seen from Figure 18b, the flow rate around the circulating pump bellmouth in Plan 10 is very uniform, and the water inlet condition of the circulating pump is better.

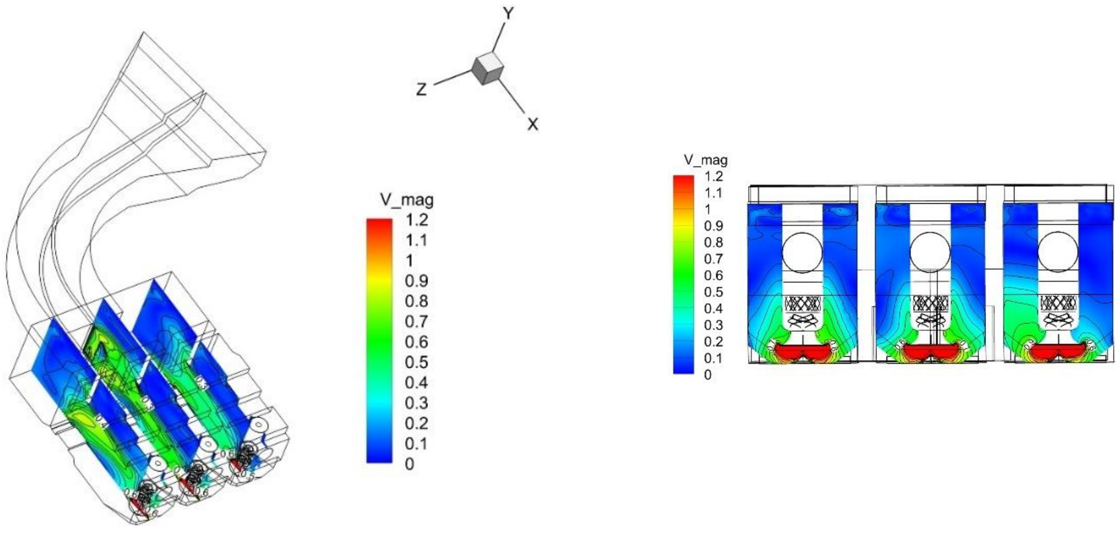

(**a**) (**b**)

Figure 17. Plan 9 Isogram of velocity. (**a**) Center section of pump body along flow direction. (**b**) Center section of pump body in vertical flow direction.

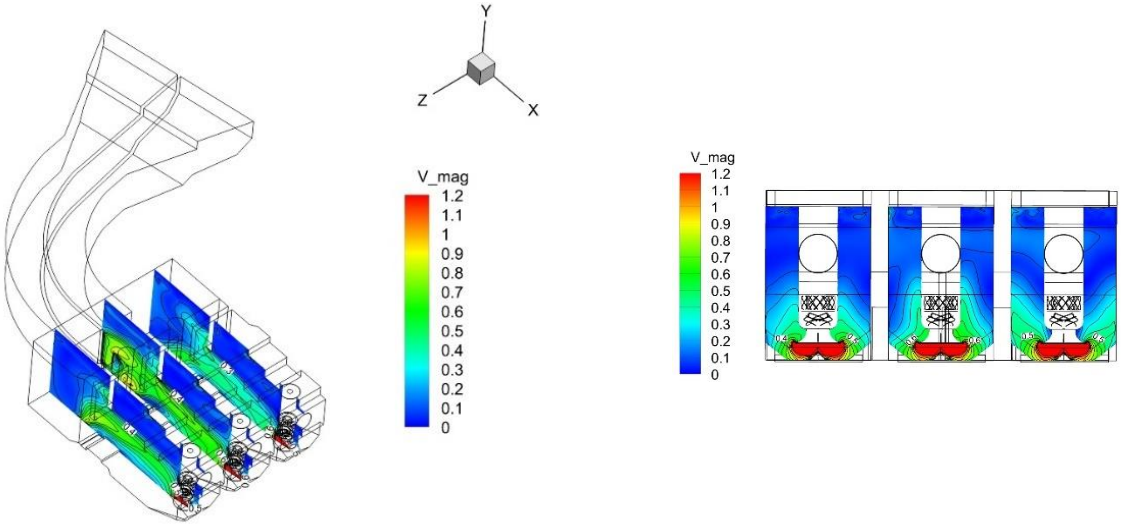

(**a**) (**b**)

Figure 18. Plan 10 isogram of velocity. (**a**) Center section of pump body along flow direction. (**b**) Center section of pump body in vertical flow direction.

5.4. Impact Analysis of Field Reconstruction

Based on the above analysis, the rectification optimization effect of Plan 10 is the best plan, so the plan is selected as the final transformation plan. At the same time, the structural degree of the construction process should be considered. Figure 19 is the construction drawing. Figure 20 is the sectional view of the foundation and the deflector. The optimal renovation plan is as follows:

(1) A straight plate with an inclination angle is set in the middle of the forebay, the length of the straight plate is 2 m, the included angle with the water flow direction is 5°, and the distance between the top of the straight board and the inlet end of the fore pool is 2 m.

(2) An arc plate is arranged on each side of the forebay, and the center of the arc is located at the wall 1 m outside the inlet end. The starting point of the arc segment is 2.67 m away from the horizontal extension line of the outer side wall of the inlet end and 2 m away from the wall at the inlet end of the front pool. The arc is 35°, and the arc radius is 4.176 m.

(3) In theory, the height of the deflector should be slightly lower than the outlet end of the forebay, but because the water flow speed gradually decreases with the increase in the height, the baffle effect is strengthened. However, the higher the height, the smaller the impact of water flow on the pump's suction port. Considering the construction volume and structural strength, the deflector height is 4 m.

(4) The thickness of the deflector is 0.2 m to 0.3 m in the simulation, and changing the thickness to a certain extent has little effect on the flow field. In the actual construction, the structural strength should be considered, and the thickness of 0.4 m should be selected, which satisfies the continuous impact of the water flow with a speed of 1.5 m/s.

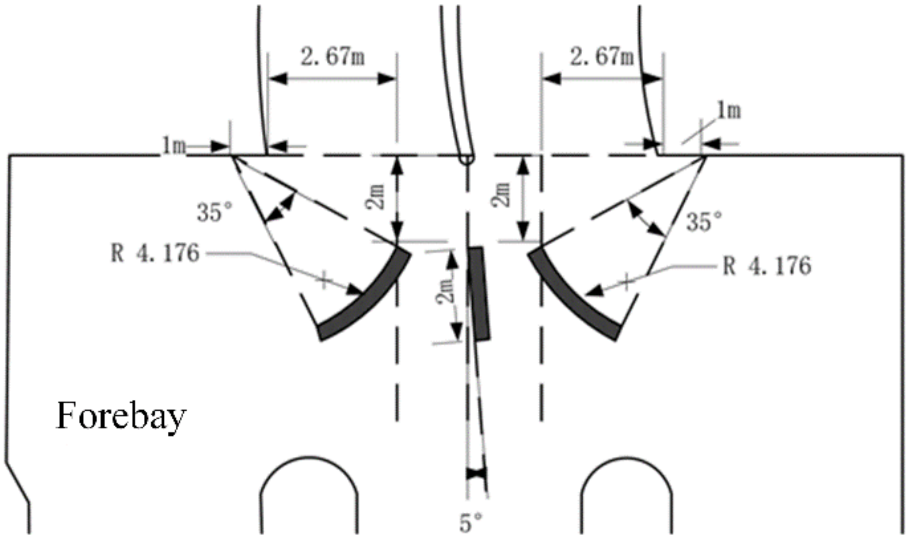

Figure 19. The construction drawing.

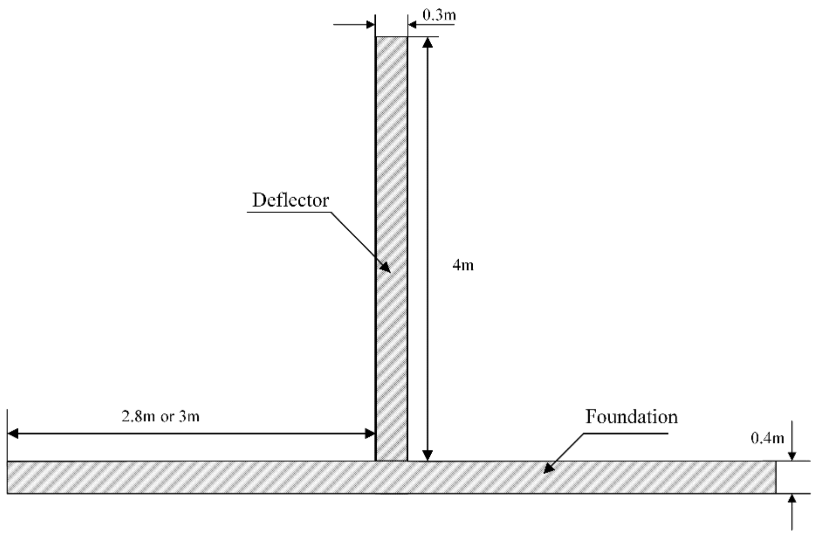

Figure 20. The sectional view of the foundation and the deflector.

During the construction, the foundation and the deflector are all made of reinforced concrete structure, the concrete material is C25 or C30, the steel material is HRB335 or HRB400, and the diameter of the steel bar is more than 16 mm. For concrete structures with a height of 4 m and below, the above materials can achieve stress balance and meet the requirements, and no verification calculation is required.

Rectification by Plan 10 completes the effect picture as shown in Figure 21. Considering the impact of high-speed water flow on the deflectors, the deflectors are connected and strengthened by channel steel. Since the channel steel structure is small, it has little influence on the flow pattern entering the water suction chamber, and the influence of channel steel structure on the simulation structure can be ignored.

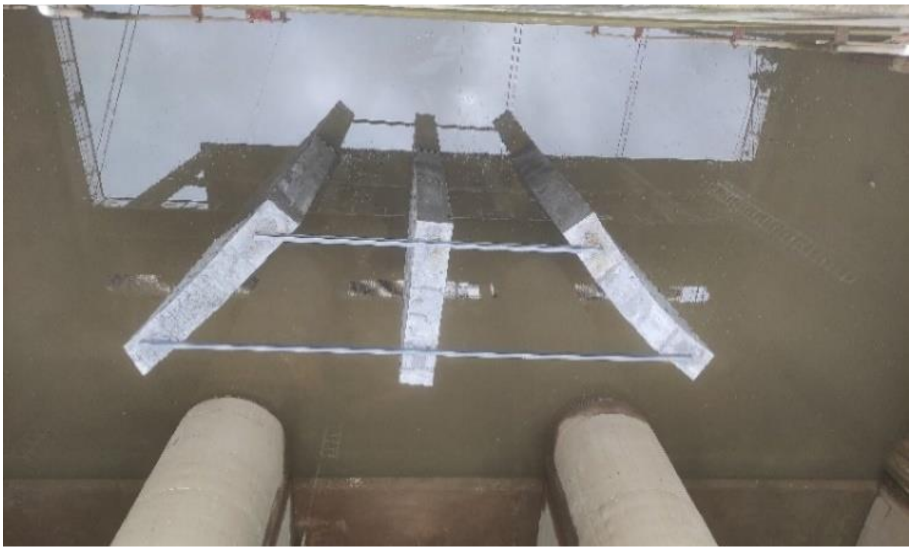

Figure 21. Completion diagram of transformation.

Before the renovation, the circulating pump had many abnormal vibrations. The operating vibration amplitude of the A circulating pump exceeded 0.22 mm, while the C circulating pump had evident vibration under low-speed conditions, and the maximum vibration amplitude was as high as 0.29 mm. Taking the C circulating pump as the representative, Table 3 shows the changes in different parameters before and after transformation. The vibration amplitude is measured by vibration sensors (CYT9200(A)), and the maximum measurement error is $\leq \pm 1\text{mm/s}$. The vibration sensor is waterproof and has a high measurement accuracy.

Table 3. Comparison of parameters before and after transformation (C circulating pump).

Performance Parameters	Flow (m^3/s)	Maximum Flow Rate (m/s)	Average Front-to-Back Velocity Difference (m/s)	Average Left–Right Velocity Difference (m/s)	Vibration Amplitude (mm)
Before	28.76	1.2	1.12	1.03	0.29
After	28.76	0.7	0.34	0.12	0.018

It can be seen from Table 3 that the flow rate has not changed before and after the transformation. The circulating pump still operates under normal working conditions after the transformation. After the arc-shaped deflector is installed in the front pool of the water inlet channel, the water flow into the suction chamber is stable, and the flow rate is low, especially the flow state at the inlet of the circulating water pump, which is greatly improved, the operating condition of the circulating water pump is better, and the abnormal vibration disappears. The three circulating pumps have been running at high speed since 1 May 2020, and no lousy vibration has occurred. The vibration amplitude of the A and C pumps is fewer than 0.02 mm, which meets the operating vibration qualification standard of 0.05 mm. The overall operation has reached an excellent level, and the transformation effect is excellent.

6. Conclusions

In this paper, the water inter channel is set up for numerical simulation, and various schemes are given to optimize the flow regime of the forebay and the suction chamber in the water channel system. Nine different plans for linear deflectors, diversion pillars, and arc deflectors are included in the corrective measures. A thorough comparison is made between the numerical simulation outcomes of various optimization measures. The best optimization plan was chosen, and the plan's implementation produced exceptional results.

(1) The forebay is constructed as an asymmetrical rectangle, per the analysis of the original operational state. The water flow cannot fully develop and diffuse because the length is too short, and the diffusion angle is too great. Following the water flow's entry into the suction chamber causes a significant drift phenomenon. The effects, as mentioned above, will lead to unequal hydraulic pressure around the circulating pump's bellmouth and body, which is likely to result in irregular vibration of the circulating pump.
(2) Different deflectors are set in the forebay to improve the variable flow, aiming at the phenomenon of water flow deviation and uneven hydraulic power. Plan 10 is the best optimization. The water flow enters from the middle of the suction chamber. The high-speed water flow and wall-adhering bias flow in the suction chamber disappear. The flow regime problem of the water inlet channel was better solved, the water inlet conditions of the bellmouth were effectively improved, and the hydraulic problem of the vibration of the circulating water pump was solved.
(3) Plan 10 is selected as the final optimization measure in the thermal power plant. The test proves that after the rectification measures are implemented, the abnormal vibration of the circulating pump unit obviously disappeared, and its operational efficiency is also improved.
(4) Numerical simulations can predict the flow patterns in the forebay and suction chamber before and after rectification, guiding the setting of reasonable rectification measures. The modification of the forebay of the power plant can provide a reference for the rectification of curved inlet channels or large diffusion angle forebays.

Author Contributions: Conceptualization, W.W. and J.Z.; methodology, W.X.; software, J.Z. and J.G.; validation, W.W. and W.X.; formal Analysis, J.Z. and Y.Z.; investigation, J.Z., J.G. and Y.Z.; resources, W.W.; data curation, J.Z. and Y.Z.; writing—original draft preparation, J.Z.; writing—review and editing, W.X.; visualization, W.W.; supervision, W.W. and W.X.; project administration, W.W. All authors have read and agreed to the published version of the manuscript.

Funding: The research was supported by the Program for Innovative Research Team (in Science and Technology) at the University of Henan Province (grant No. 16IRTSTHN017).

Institutional Review Board Statement: Not applicable.

Informed Consent Statement: Not applicable.

Data Availability Statement: The data that support the findings of this study are available from the corresponding author upon reasonable request.

Conflicts of Interest: The authors declare that there is no conflict of interest regarding the publication of this paper.

References

1. Liu, J.; Qu, B.; Zhang, Z. Energy analysis of centralized circulating cooling water system. *Water Resour. Power* **2017**, *35*, 161–164.
2. Gao, C.; Zeng, X.; Xie, K.; Tang, L. Combined rectification scheme of pump intake sump in ultra-low water level and its verification. *Trans. Chin. Soc. Agric. Eng.* **2017**, *33*, 101–108.
3. Wang, F.; Tang, X.; Chen, X. A review on flow analysis method for pumping stations. *J. Hydraul. Eng.* **2018**, *49*, 47–61.
4. Xu, C.; Zhang, H.; Zhang, X. Numerical simulation of the impact of unit commitment optimization and divergence angle on the flow pattern of forebay. *Int. J. Heat Technol.* **2015**, *33*, 91–96. [CrossRef]
5. Kim, C.G.; Kim, B.H.; Bang, B.H. Experimental and CFD analysis for prediction of vortex and swirl angle in the pump sump station model. In Proceedings of the International Symposium of Cavitation and Multiphase Flow, Beijing, China, 18–21 October 2014.
6. Xu, W.; He, X.; Hou, X. Influence of Wall Roughness on Cavitation Performance of Centrifugal Pump. *J. Braz. Soc. Mech. Sci. Eng.* **2021**, *43*, 314. [CrossRef]
7. Luo, C.; Cheng, L.; Liu, C. Numerical simulation of mechanism for sill rectifying flow in pumping station intake. *J. Drain. Irrig. Mach. Eng.* **2014**, *32*, 393–398.
8. Han, J.; Li, Y.; Gao, D. 3D Numerical simulation and optimum design of circulating water pump flow channel in thermal plant. *Yellow River* **2012**, *34*, 143–145+148.
9. Zhou, J.; Zhong, Z.; Liang, J. Three-dimensional Numerical Simulation of Side-intake Forebay of Pumping Station. *J. Irrig. Drain* **2015**, *34*, 52–55.

10. Xu, C.; Wang, R.; Li, H.; Zhang, R.; Wang, M.; Wang, Y. Flow pattern and anti-silt measures of straight-edge forebay in large pump stations. *Heat Technol.* **2018**, *36*, 1130–1139. [CrossRef]
11. Cheng, L.; Chao, L.; Jiren, Z. Discussion on the Side-direction Flow of Pumping Station and Improving of the Flow Pattern. *Drain. Irrig. Mach.* **2001**, *19*, 31–34.
12. Wang, X.; Guo, F. Experimental Research on the Hydraulic Characteristics of the Pumping Stations Forebay. *Water Conserv. Sci. Technol.* **2006**, *9*, 597–598.
13. Liu, X.; Gao, C.; Shi, L. Numerical simulation for fluid meliorating in both forebay and suction bay of pump stations. *J. Drain. Irrig. Mach. Eng.* **2010**, *28*, 242–246.
14. Yang, F.; Zhang, Y.; Liu, C. Numerical and Experimental Investigations of Flow Pattern and Anti-Vortex Measures of Forebay in a Multi-Unit Pumping Station. *Water* **2021**, *13*, 935. [CrossRef]
15. Ying, J.; Yu, X.; He, W. Volume of fluid model-based flow pattern in forebay of pump station and combined rectification plan. *J. Drain. Irrig. Mach. Eng. (JDIME)* **2020**, *38*, 476–480.
16. Xu, R.; Xu, L.; Lu, L. Optimum design of rectifying flow of diversion pillar array in pressure forebay with extra-large diffusion angle of a pumping station. *Water Resour. Hydropower Eng.* **2021**, *52*, 134–145.
17. Bai, Y.; Li, B.; Xu, H. Rectification analysis of multi-person diversion pier in large-span pumping station. *Water Resour. Power* **2019**, *37*, 75–79.
18. Long, Z.; Xiao, L.; Yuan, S. Numerical Simulation of Turbulent Flow in Recycled Water Pump Intake Sump of Thermal Power Plant. In Proceedings of the 2009 Asia-Pacific Power and Energy Engineering Conference, Wuhan, China, 27–31 March 2009.